Recovery of Raman spectra with low signal-to-noise ratio using Wiener estimation

Chen, Shuo; Lin, Xiaoqian; Yuen, Clement; Padmanabhan, Saraswathi; Beuerman, Roger W.; Liu, Quan

2014

Chen, S., Lin, X., Yuen, C., Padmanabhan, S., Beuerman, R. W., & Liu, Q. (2014). Recovery of Raman spectra with low signal-to-noise ratio using Wiener estimation. Optics Express, 22(10), 12102-12114 .

https://hdl.handle.net/10356/80910

https://doi.org/10.1364/OE.22.012102

Recovery of Raman spectra with low signal-to-noise ratio using Wiener estimation

Shuo Chen,[1] Xiaoqian Lin,[1] Clement Yuen,[1] Saraswathi Padmanabhan,[2] Roger W. Beuerman,[2] Quan Liu[1,*]

[1]*Nanyang Technological University, Division of Bioengineering, School of Chemical and Biomedical Engineering, 637457, Singapore*
[2]*Singapore Eye Research Institute, 11 Third Hospital Avenue, 168751, Singapore*
*quanliu@ntu.edu.sg

Abstract: Raman spectroscopy is a powerful non-destructive technique for qualitatively and quantitatively characterizing materials. However, noise often obscures interesting Raman peaks due to the inherently weak Raman signal, especially in biological samples. In this study, we develop a method based on spectral reconstruction to recover Raman spectra with low signal-to-noise ratio (SNR). The synthesis of narrow-band measurements from low-SNR Raman spectra eliminates the effect of noise by integrating the Raman signal along the wavenumber dimension, which is followed by spectral reconstruction based on Wiener estimation to recover the Raman spectrum with high spectral resolution. Non-negative principal components based filters are used in the synthesis to ensure that most variance contained in the original Raman measurements are retained. A total of 25 agar phantoms and 20 bacteria samples were measured and data were used to validate our method. Four commonly used de-noising methods in Raman spectroscopy, i.e. Savitzky-Golay (SG) algorithm, finite impulse response (FIR) filtration, wavelet transform and factor analysis, were also evaluated on the same set of data in addition to the proposed method for comparison. The proposed method showed the superior accuracy in the recovery of Raman spectra from measurements with extremely low SNR, compared with the four commonly used de-noising methods.

OCIS codes: (170.5660) Raman spectroscopy; (300.6450) Spectroscopy, Raman; (300.6170) Spectra.

References and links

1. Y. H. Ong, M. Lim, Q. Liu, "Comparison of principal component analysis and biochemical component analysis in Raman spectroscopy for the discrimination of apoptosis and necrosis in K562 leukemia cells," Opt. Express **20**, 22158-22171 (2012).
2. Y. Li, J. Pan, G. Chen, C Li, S. Lin, Y. Shao, S. Feng, Z. Huang, S. Xie, H. Zeng, R. Chen, "Micro-Raman spectroscopy study of cancerous and normal nasopharyngeal tissues," J. Biomed. Opt. **18**, 027003-027003 (2013).
3. A. E. Kandjani, M. J. Griffin, R. Ramanathan, S. J. Griffin, S. K. Bhargava, V. Bansal, "A new paradigm for signal processing of Raman spectra using a smoothing free algorithm: Coupling continuous wavelet transform with signal removal method," J. Raman Spectrosc. **44**, 608-621 (2013).
4. S. Feng, J. Lin, Z. Huang, G. Chen, W. Chen, Y. Wang, R. Chen, H. Zeng, "Esophageal cancer detection based on tissue surface-enhanced Raman spectroscopy and multivariate analysis," Appl. Phys. Lett. **102**, 043702-043702-4 (2013).
5. J. Lin, R. Chen, S. Feng, J. Pan, B. Li, G. Chen, S. Lin, C. Li, L. Sun, Z. Huang, H. Zeng, "Surface-enhanced Raman scattering spectroscopy for potential noninvasive nasopharyngeal cancer detection," J. Raman Spectrosc. **43**, 497-502 (2012).
6. G. Li, "Noise Removal of Raman Spectra Using Interval Thresholding Method." in *Proceeding of IEEE conference on Intelligent Information Technology Application (Shanghai, 2008),* pp. 535-539.
7. M. Člupek, P. Matějka, K. Volka, "Noise reduction in Raman spectra: Finite impulse response filtration versus Savitzky–Golay smoothing," J. Raman Spectrosc. **38**, 1174-1179 (2007).

8. A. Kwiatkowski, M. Gnyba, J. Smulko, P. Wierzba, "Algorithms of chemicals detection using raman spectra," Metrol. Meas. Syst. **17**, 549-559 (2010).
9. M. Villarroel, P. Barreiro, P. Kettlewell, M. Farish, M. Mitchell, "Time derivatives in air temperature and enthalpy as non-invasive welfare indicators during long distance animal transport," Biosyst. Eng. **110**, 253-260 (2011).
10. Y.P. Wang, Y. Wang, P. Spencer, "Fuzzy clustering of Raman spectral imaging data with a wavelet-based noise-reduction approach," Appl. Spectrosc. **60**, 826-832 (2006).
11. F. Ehrentreich and L. Sümmchen, "Spike Removal and Denoising of Raman Spectra by Wavelet Transform Methods," Anal. Chem. **73**, 4364-4373 (2001).
12. J. Palacký, P. Mojzeš, J. Bok, "SVD-based method for intensity normalization, background correction and solvent subtraction in Raman spectroscopy exploiting the properties of water stretching vibrations," J. Raman Spectrosc. **42**, 1528-1539 (2011).
13. J. Hanuš, K. Chmelová, J. Štěpánek, P. Y. Turpin, J. Bok, I. Rosenberg, Z. Točík, "Raman spectroscopic study of triplex-like complexes of polyuridylic acid with the isopolar, non-isosteric phosphonate analogues of diadenosine monophosphate," J. Raman Spectrosc. **30**, 667-676 (1999).
14. S. Chen, Y. H. Ong, Q. Liu, "Fast reconstruction of Raman spectra from narrow-band measurements based on Wiener estimation," J Raman Spectrosc. **44**, 875-881 (2013).
15. S. Chen and Q. Liu, "Modified Wiener estimation of diffuse reflectance spectra from RGB values by the synthesis of new colors for tissue measurements," J Biomed. Opt. **17**, 030501-1-030501-3 (2012).
16. H. Haneishi, T. Hasegawa, A. Hosoi, Y. Yokoyama, N. Tsumura, Y. Miyake, "System design for accurately estimating the spectral reflectance of art paintings," Appl. Opt. **39**, 6621-6632 (2000).
17. W. F. Zhang and D. Q. Dai, "Spectral reflectance estimation from camera responses by support vector regression and a composite model," J. Opt. Soc. Am. A **25**, 2286-2296 (2008).
18. R. Piché, "Nonnegative color spectrum analysis filters from principal component analysis characteristic spectra," J. Opt. Soc. Am. A **19**, 1946-1950 (2002).
19. J. S. U. Hjorth, "Cross validation," in *Computer intensive statistical methods: validation, model selection, and boostrap* (Chapman and Hall/CRC, 1993).
20. P. Martinez, "Bias," in *A practical guide to CCD astronomy* (Cambridge University, 1998, 8).
21. R. L. McCreery, "SNR," in *Raman spectroscopy for chemical analysis* (John Wiley & Sons, 2005, 157).
22. D. Chen, Z. Chen, E. Grant, "Adaptive wavelet transform suppresses background and noise for quantitative analysis by Raman spectrometry," Anal. Bioanal Chem. **400**, 625-634 (2011).
23. B. Hu, Q. Li, A. Smith, "Noise reduction of hyperspectral data using singular spectral analysis," Int. J. Remote Sens. **30**, 2277-2296 (2009).
24. L. Birgé and P. Massart, "Birge-Massart strategy," in *Research papers in probaility and statistics* (Springer, 1997, 35).
25. Z. Huang, A. McWilliams, H. Lui, D. McLean, S. Lam, H. Zeng, "Near-infrared Raman spectroscopy for optical diagnosis of lung cancer," Int. J. Cancer **107**, 1047-1052 (2003).
26. P. M. Ramos and I. Ruisánchez, "Noise and background removal in Raman spectra of ancient pigments using wavelet transform," J. Raman Spectrosc. **36**, 848-856 (2005).
27. D. Van de Sompel, E. Garai, C. Zavaleta, S. S. Gambhir, "A comparison of noise models in a hybrid reference spectrum and principal components analysis algorithm for Raman spectroscopy," J. Raman Spectrosc. **44**, 841-856 (2013).
28. J. M. Williamson, R. J. Bowling, R. L. McCreery, "Near-Infrared Raman Spectroscopy with a 783-nm Diode Laser and CCD Array Detector," Appl. Spectrosc. **43**, 372-375 (1989).
29. J. Khan, J. S. Wei, M. Ringner, L. H. Saal, M. Ladanyi, F. Westermann, F. Berthold, M. Schwab, C. R. Antonescu, C. Peterson, P. S. Meltzer, "Classification and diagnostic prediction of cancers using gene expression profiling and artificial neural networks," Nat. Med. **7**, 673-679 (2001).
30. F. Harrell Jr, K. Lee, D. Mark, "Multivariable prognostic models: issues in developing models, evaluating assumptions and adequacy, and measuring and reducing errors," Stat. Med. **15**, 361 (1996).
31. H. G. Schulze, R. B. Foist, A. Ivanov, R. F. Turner, "Fully automated high-performance signal-to-noise ratio enhancement based on an iterative three-point zero-order Savitzky-Golay filter," Appl. Spectrosc. **62**, 1160-1166 (2008).
32. H. G. Schulze, R. B. Foist, A. Ivanov, R. F. Turner, "Chi-squared-based filters for high-fidelity signal-to-noise ratio enhancement of spectra," Appl. Spectrosc. **62**, 847-853 (2008).
33. R. B. Foist, H. G. Schulze, A. Jirasek, A. Ivanov, R. F. Turner, "A matrix-based two-dimensional regularization algorithm for signal-to-noise ratio enhancement of multidimensional spectral data," Appl. Spectrosc. **64**, 1209-1219 (2010).

1. Introduction

Raman spectroscopy is a laser-based spectroscopic technique that exploits Raman scattering for qualitative or quantitative biological material characterization [1]. Rich biochemical information can be revealed from resulting Raman shifts, which depend on the specific

vibrational modes of molecules in tissues and cells [2]. Therefore, Raman spectra or peaks inside could be employed to differentiate biological components. This method has shown great potential in many biomedical applications [3, 4]. Unfortunately, such applications are often hampered by inherently weak Raman signals from biological molecules [5]. In this case, measurement noises obscure Raman peaks of interest rendering a low signal-to-noise ratio (SNR) [6]. It is common to solve this problem by increasing the power of the excitation laser and/or exposure time. However, these methods cannot be used when measuring unstable materials or observing fast changing phenomena. Therefore, it is important to develop a method to quickly recover Raman spectra with low SNR without increasing laser power.

Smoothing and filtering are two common categories of de-noising methods in Raman spectroscopy [7]. Savitzky-Golay (SG) algorithm is one of the most frequently used smoothing methods to de-noise Raman spectra [8], in which each segment of the original Raman spectrum in a small window is smoothed by fitting it to a polynomial function [9]. When the window size is small, the smoothing outcome will be poor. When the window size is large, the spectral resolution will degrade and those weak spectral features will be distorted. A tradeoff needs to be made between the smoothing outcome and the spectral resolution by appropriately choosing the window size and the order of the polynomial function. In contrast, finite impulse response (FIR) filtration [7], wavelet transform [10, 11] and factor analysis [12], are commonly used filtering techniques for Raman de-noising. FIR filtration offers excellent preservation of the spectral shape, but it is demanding in computation. In the technique of wavelet transform, spectral data are decomposed into the wavelet domain and reconstructed after thresholding for noise removal. Currently, the selection of wavelet filters, threshold and other parameters in wavelet transform is strongly problem dependent [11]. In factor analysis, acquired spectra are projected into the orthonormal set of subspectra by singular value decomposition. The original spectral information is maintained by the linear combination of optimized number of subspectra with large singular values. The subspectra with small singular values (usually below 0.5% of the maximal value) are treated as white noise [13]. The method will lose the ability to decompose the signal and the noise when the SNR is low, because the noise would have comparable or even more contribution to the acquired spectra compared to the signal.

In our previous study [14], we have successfully reconstructed the Raman spectra of cells and biological fluid from narrow-band measurements using the WE method without sacrificing spectral resolution. In this study, we propose the reconstruction of Raman spectra from narrow-band measurements based on Wiener estimation (WE) method as an alternative method to denoise Raman spectra with low SNR. By synthesizing narrow-band measurements from low-SNR spectra, the integration along the wavenumber dimension in the synthesis reduces the effect of noise. Then the narrow-band measurements are used to reconstruct high-SNR spectra based on Wiener estimation. To our best knowledge, this is the first time that spectral reconstruction involving Wiener estimation is used to recover the high-SNR Raman spectra from narrow-band measurements that were synthesized from low-SNR Raman measurements. Although traditional Wiener filtration for noise reduction and spectral reconstruction based on Wiener estimation have been performed separately before, our method is different from either one of them. In traditional Wiener filtration, narrow-band measurements are never synthesized and the Wiener filter is directly applied to a signal with the additive noise. In the traditional spectral reconstruction based on Wiener estimation, there is no previous study in which narrow-band measurements are synthesized from low-SNR Raman spectra to recover the corresponding high-SNR Raman spectra. So the traditional spectral reconstruction based on Wiener estimation is not able to de-noise the spectra.

More specifically, we systematically investigated the recovery of Raman spectra from Raman measurements with low SNR obtained by using a series of short exposure time values during spectral acquisition, in which Raman spectra with high SNR obtained using a long exposure time served as the reference measurement for comparison. Narrow-band measurements synthesized from Raman spectra with low SNR using a set of non-negative principal components (PCs) based filters were used to reconstruct Raman spectra with high

SNR by Wiener estimation. The choice of non-negative PCs based filters in the process ensures that most variance contained in the original Raman measurements are retained. The method was validated on Raman spectra measured from 25 phantoms with two different Raman scatterers, i.e. urea and potassium formate, at different concentrations and 20 Raman spectra measured from bacteria samples. Four commonly used Raman de-noising methods, i.e. SG algorithm, FIR filtration, wavelet transform and factor analysis, were evaluated on the same sets of Raman spectra for comparison. According to the results, the agreement between the Raman spectra recovered by WE method and the reference Raman spectra was significantly better than the four common de-noising methods. Therefore our method represents an effective alternative to recover Raman spectra from samples with intrinsically low Raman efficiency or those acquired in short time from fast changing phenomena thus with low SNR.

2. Materials and Methods

2.1 Principle of Wiener estimation for recovery of Raman spectra

Wiener estimation [15, 16] is used to recover Raman spectra from low-SNR Raman measurements and results are compared to the reference Raman spectra with high SNR. The low SNR Raman measurements are collected from a sample with short exposure time and single accumulation, while the corresponding reference Raman spectra with high SNR are collected from the same sample with long exposure time and multiple accumulations.

In the recovery process, there are two data sets involved, i.e. the calibration data set and test data set. The calibration data set contains both Raman measurements with low SNR and the corresponding reference Raman measurements with high SNR. In the test data set, only Raman measurements with low SNR are present.

The role of the calibration data set is to yield the Wiener matrix [17] when ignoring noise term according to Eq. (1) below.

$$\mathrm{W} = \mathrm{E}(S_{high} C_{cal}^{T})[\mathrm{E}(C_{cal} C_{cal}^{\mathrm{T}})]^{-1} \tag{1}$$

where W is the Wiener matrix, S_{high} is the reference Raman measurements with high SNR and C_{cal} is the narrow-band measurements synthesized from Raman measurements with low SNR in the calibration data set.

Narrow-band measurements C_{cal} are synthesized from the Raman measurements with low SNR in the calibration data set using non-negative PCs based filters that were generated using a published method [18] according to Eq. (2) below.

$$C = FS_{low} \tag{2}$$

where C (n×1 matrix) is the synthesized narrow-band measurements, F (n×m matrix) is the transmission spectrum of non-negative PCs based filters and S_{low} (m×1 matrix) is the Raman spectrum with low SNR. Note that m is the number of discrete wavenumbers in the Raman spectrum and n is the number of filters in synthesized narrow-band measurements.

Then the recovery of Raman spectra from a set of Raman measurements with low SNR in the test data set is achieved according to Eq. (3) below.

$$\hat{S}_{high} = WC_{test} \tag{3}$$

where $\hat{S}_{high}$ (m×1) is the recovered Raman spectrum with high SNR and C_{test} is the narrow-band measurements synthesized according to Eq. (2) from Raman measurements with low SNR in the test data set.

The leave-one-out method [19] is used for cross validation in our study to fully utilize all samples in an unbiased manner. In this strategy, one sample is selected as the test data set and

the rest of samples serve as the calibration data set. The procedure is repeated until all the samples have been tested.

2.2 Sample preparation and measurements

Two sets of samples were used to validate our method, which includes 25 phantom samples and 20 bacteria samples. The tunability in the composition of phantoms and the concentration of each Raman scatterer in the phantoms makes the phantom study ideal in quantitative evaluation. Bacteria samples were used because the Raman signal from bacteria is weak even with a long exposure time thus it is an excellent target to demonstrate the effectiveness of the recovery of Raman spectra with low SNR using the proposed method.

The phantoms were made by mixing urea (V3171, Promega corporation, US) and potassium formate (294454-500G, Sigma-Aldrich, US) in 1.5% agar (PC0701-500G, Vivantis Technologies, US) dissolved in distilled water. The concentrations for both urea and potassium formate under investigation included 0.25 M, 0.5 M, 1 M, 1.5 M and 2 M. Raman spectra with both low SNR and high SNR were measured over a range from 600 cm^{-1} to 1800 cm^{-1}, by using a micro-Raman system (innoRam-785S, B&W TEK, US) coupled to a video microscope sampling system (BAC151A, B&W TEK, US). The excitation wavelength was 785 nm and the spectral resolution was 4 cm^{-1}. The exposure time for Raman spectra with low SNR was 50 ms and each spectrum was accumulated for once, while the exposure time for Raman spectra with high SNR was 10 s and each spectrum was accumulated for 30 times.

The bacterial samples, including *Pseudomonas aeruginosa* (ATCC 9027) and *Staphylococcus aureus* (ATCC 29213), was grown overnight in Tryptic Soy Agar Plates (TSA) at 35 °C. Few colonies were picked up and suspended in Phosphate Buffered Saline (PBS) to a concentration of 1×10^8 CFU/ml, which were then concentrated by centrifuging at 10,000 rpm for five minutes and the supernatant was discarded. After that, the bacteria sample was washed twice in 1 mL distilled water to remove any culture media and finally suspended in 100 μL distilled water. The suspended samples with a volume of 2 μL were repeatedly dropped at the same position on an aluminum foil for five or ten times to create rounded areas with different bacteria concentrations. Five pairs of Raman spectra, one with low SNR and the other with high SNR in each pair, were measured over a range from 600 cm^{-1} to 1600 cm^{-1} from five different locations in each rounded area. Among these five locations picked randomly, three of them were located at the edge and two at the center of the drop in each rounded area to account for the variability in bacteria concentration. This procedure of sample preparation and Raman measurements were repeated for a total of four times to generate 20 pairs of Raman spectra. Raman measurements were performed using a micro-Raman system (inVia, Renishaw, UK) coupled to a microscope (Alpha 300, WITec, Germany) in a backscattering setup. The excitation wavelength was 633 nm and the spectral resolution was 2 cm^{-1}. The exposure time for Raman spectra with low SNR was 1 s and each spectrum was accumulated for once only, while the exposure time for Raman spectra with high SNR was 10 s and each spectrum was accumulated for 30 times. In addition, Raman spectra with an exposure time of 5 s or 10 s and accumulation of once were measured for comparison.

In order to quantify the noise level of the Raman spectra with low SNR in this study, the SNR was defined as follows in Eq. (4).

$$\mathrm{SNR} = \frac{s}{\sigma} \tag{4}$$

where s is the largest peak intensity of the reference Raman spectrum (with high SNR) divided by a scaling coefficient and σ is the root mean square deviation between the low-SNR Raman spectrum and the scaled reference Raman spectrum in the entire spectral range. The scaling coefficient is obtained by dividing the sum of all the intensity values in the reference Raman spectrum by that in the corresponding low-SNR Raman spectrum. Due to the significant pixel bias, which refers to the detector reading independent of exposure time [20], of the Raman system used in phantom experiments, pixel bias correction was conducted in

phantom spectra before SNR calculation. Note that the pixel bias issue was insignificant in the Raman system used in bacteria measurements thus no correction was performed before SNR calculation for the bacteria data. The pixel bias value for any given phantom spectrum was extracted from the linear fitting between the sums of all intensity values in the reference Raman spectra and those in the corresponding low SNR Raman spectra. The traditional SNR is equivalent to the average peak height (usually above the baseline) divided by the standard deviation of the peak height [21]. The numerator, s, in Eq. (4) is the same as the average peak height in the traditional definition of SNR. The denominator of Eq. (4), σ, is equivalent to the standard deviation of the peak height in the traditional SNR because the peak intensity is nearly on the same level as the background intensities in low-SNR Raman measurements as shown in Fig. 1(a) and 2(a).

2.3 Evaluation of SG algorithm, FIR filtration, wavelet transform and factor analysis

Four de-noising methods were used to recover Raman spectra from low-SNR Raman measurements for comparison. Optimal accuracy was found by selecting the best combination of parameters. For SG algorithm, the frame size was varied from 3 to the maximum odd number that was smaller than or equal to the number of data points in each spectrum. The polynomial degree was varied from 1 to 9. For FIR filtration, the window size was varied from 2 to an integer smaller than or equal to 1/3 of the number of data points in each spectrum and the cutoff frequency was ranged from 1×10^{-10} to 1. For wavelet transform, although there exist improved wavelet transform methods [10, 22], the relevant codes are not publically available. Therefore only the basic wavelet transform, which can be implemented using built-in functions in Matlab, was used. Common wavelet filters built in Matlab were tested and the level of decomposition was varied from 1 to 10. The thresholds were selected according to Birge-Massart strategy [23, 24] and both soft and hard thresholding were evaluated. For factor analysis, the number of subspectra used for linear combination was varied from 1 to the maximum value possible [12, 13].

The criterion used to define the accuracy of recovered Raman spectra in this study was the relative root mean square error (RMSE), which was formulated as in Eq. (5)

$$\text{Relative RMSE} = \left[\frac{\sum_{i=1}^{N} [R_{low}(\lambda_i) - R_{high}(\lambda_i)]^2}{N \times \{\max[R_{high}(\lambda_i)]\}^2} \right]^{1/2} \tag{5}$$

where R_{low} is the Raman signal (normalized with or without removing fluorescence background) reconstructed from the measured Raman spectrum S_{low} using Wiener estimation as shown in Eqs. (1)-(3), R_{high} is the Raman signal (normalized with or without removing fluorescence background) computed from the reference Raman signal S_{high}, λ_i is the i-th wavenumber (i is varied from 1 to N) and the function max[] returns the maximum intensity in the input spectrum. The fluorescence background was removed by fitting the original spectrum to the fifth order polynomial and subtracting the fitted spectrum from the original one [25]. The spectrum was then normalized by dividing the intensity at each wavenumber by the sum of the intensities at all wavenumbers.

3. Results

Fig. 1 shows (a) Raman spectra with low SNR, (b) reference Raman spectra with high SNR measured from phantoms and (c) first three non-negative PCs based filters generated from the reference Raman spectra. Fig. 2 shows (a) Raman spectra with low SNR, (b) reference Raman spectra with high SNR measured from bacteria samples and (c) first six non-negative PCs based filters generated from the reference Raman spectra. It should be noted that these are raw spectra without going through background removal. For both phantoms and bacteria samples, the Raman spectra with low SNR are much noisier than reference Raman spectra and Raman

peaks are overwhelmed by noise. The mean SNR of Raman spectra with low SNR for phantom samples is 6.02, while the mean SNR of Raman spectra with low SNR for bacteria samples is 0.98. Although the exposure time for bacteria samples (1 s) is longer than the exposure time for phantoms (50 ms), the bacteria samples show worse SNR due to the intrinsically weak Raman signal from bacteria.

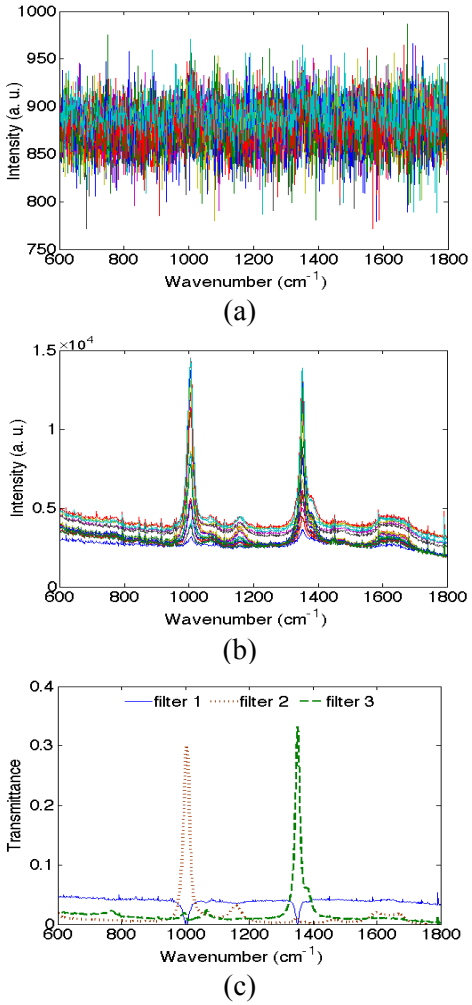

Fig. 1. (a) Raman spectra with low SNR and (b) reference Raman spectra with high SNR measured from 25 phantoms and (c) non-negative PCs based filters' transmittance spectra

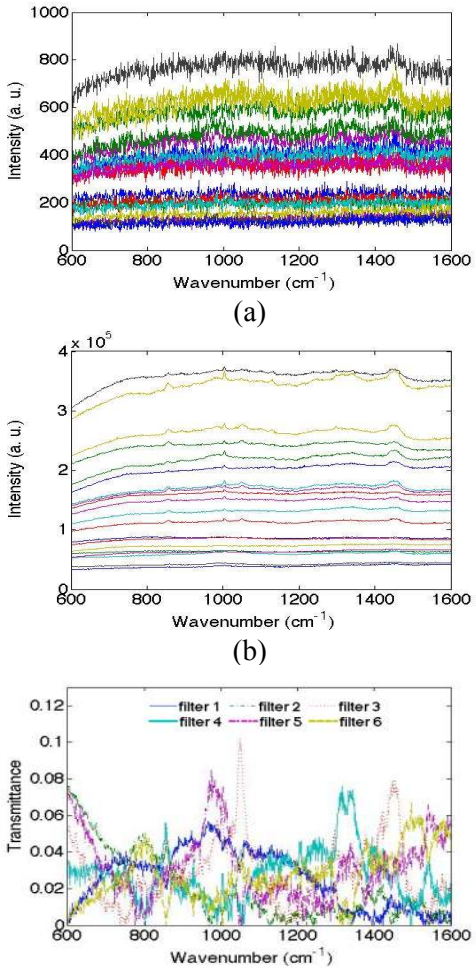

Fig. 2. (a) Raman spectra with low SNR (b) reference Raman spectra with high SNR measured from bacteria samples and (c) non-negative PCs based filters' transmittance spectra

Table 1. Comparison in the mean relative RMSE of Raman spectra of phantoms (after fluorescence background removal and normalization) recovered/smoothed from low-SNR Raman measurements using SG algorithm, FIR filtration, wavelet transform, factor analysis and WE method

	SG algorithm	FIR filtration	Wavelet transform	Factor analysis	WE method
Mean relative RMSE	1.07×10^{-1}	1.09×10^{-1}	1.02×10^{-1}	1.06×10^{-1}	1.99×10^{-2}

Table 1 shows the comparison in the mean relative RMSE of reconstructed/smoothed Raman spectra (after removing fluorescence background and normalization as described in the Materials and Methods section) from phantoms using SG algorithm, FIR filtration, wavelet transform, factor analysis and WE method. The mean relative RMSE for WE method is only 18.6%, 18.3%, 19.5% and 18.8% of those for SG algorithm, FIR filtration, wavelet transform and factor analysis, respectively. Fig. 3 shows the comparison of the reference Raman spectrum and the Raman spectra recovered/smoothed from low-SNR Raman measurements

using SG algorithm, FIR filtration, wavelet transform, factor analysis and WE method in the typical case, in which the relative RMSE is close to the mean value.

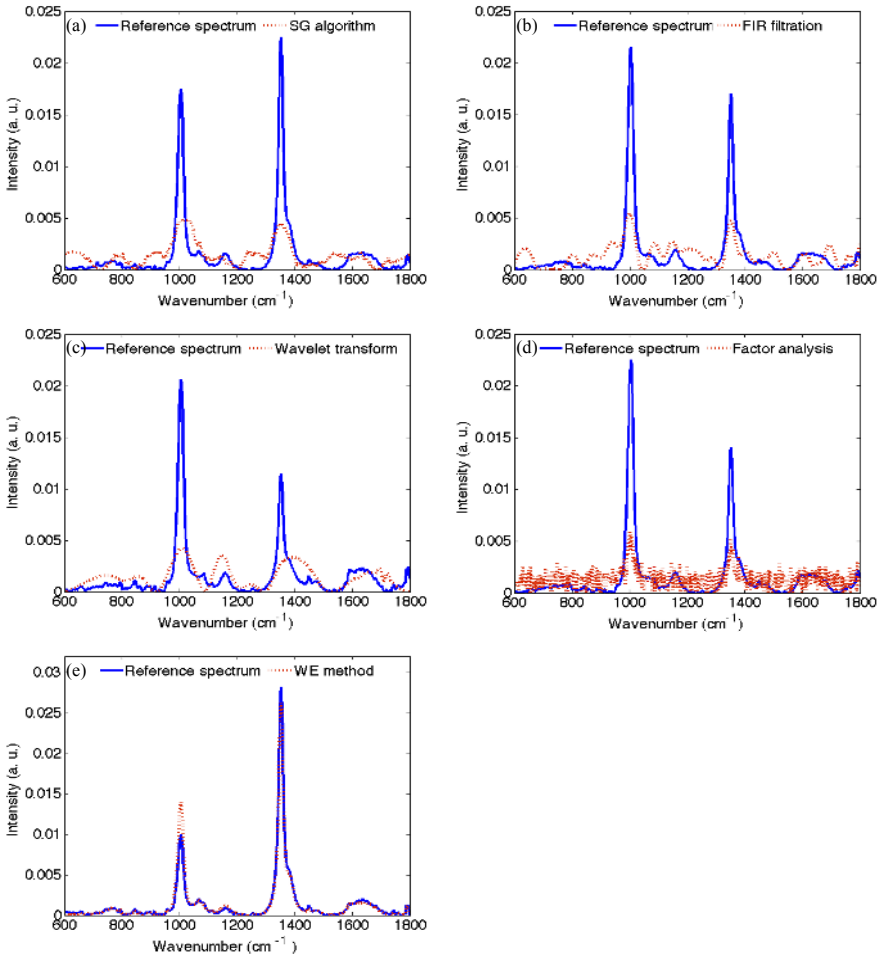

Fig. 3. Comparison of the reference Raman spectra from phantoms and the corresponding spectra recovered from low-SNR Raman measurements using (a) SG algorithm, (b) FIR filtration method, (c) wavelet transform, (d) factor analysis and (e) WE method, in which the relative RMSE is close to the mean value. Fluorescence background has been removed and spectra have been normalized.

Table 2. Comparison in the mean relative RMSE of Raman spectra of bacteria samples (after fluorescence background removal and normalization) recovered/smoothed from low-SNR Raman measurements using SG algorithm, FIR filtration, wavelet transform, factor analysis and WE method

	SG algorithm	FIR filtration	Wavelet transform	Factor analysis	WE method
Mean relative RMSE	1.47×10^{-1}	1.54×10^{-1}	1.45×10^{-1}	1.48×10^{-1}	8.21×10^{-2}

Table 2 shows the comparison in the mean relative RMSE of Raman spectra (after fluorescence background removal and normalization) from bacteria samples recovered using SG algorithm, FIR filtration, wavelet transform, factor analysis and WE method. The mean relative RMSE for WE method is 55.9%, 53.3%, 56.6%, 55.5% those of SG algorithm, FIR filtration, wavelet transform and factor analysis, respectively. Fig. 4 shows the comparison of

the reference Raman spectra and the corresponding spectra recovered/smoothed using SG algorithm, FIR filtration, wavelet transform, factor analysis and WE method, in which the relative RMSE is close to the mean value.

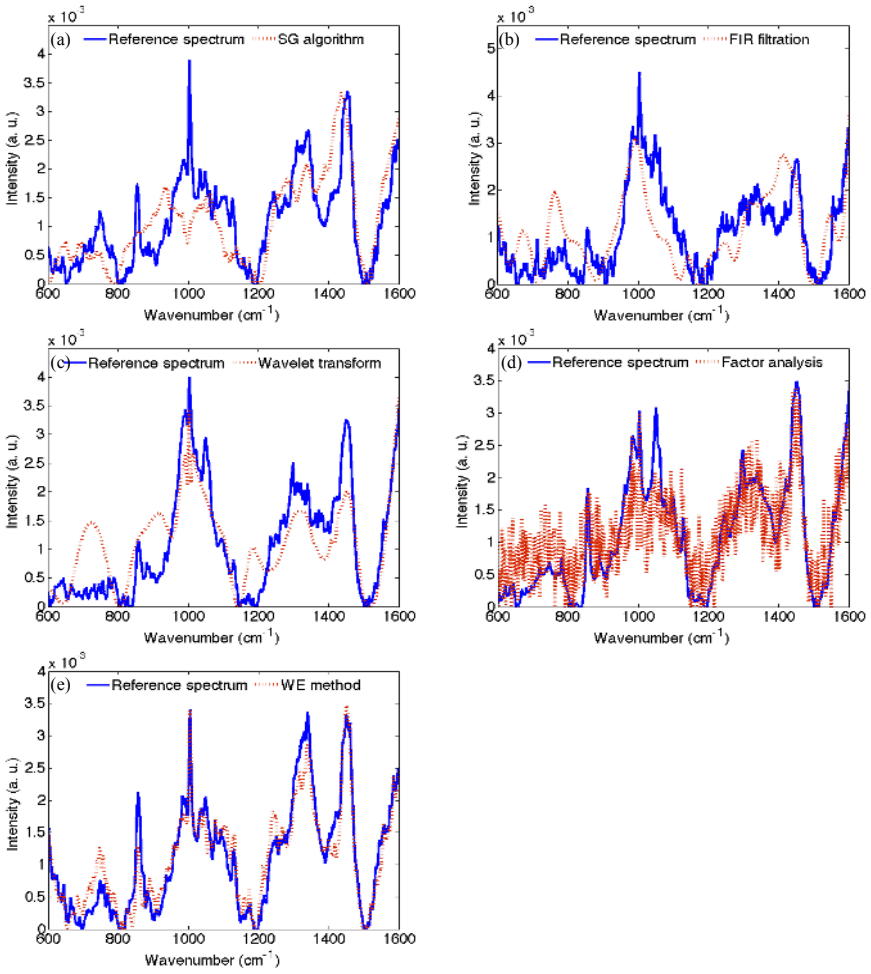

Fig. 4. Comparison of the reference Raman spectra from bacteria samples and the Raman spectra recovered from low-SNR Raman measurements using (a) SG algorithm, (b) FIR filtration method, (c) wavelet transform, (d) factor analysis and (e) WE method, in which the relative RMSE is close to the mean value. Fluorescence background has been removed and spectra have been normalized.

Table 3. Comparison in the mean relative RMSE of Raman spectra of phantoms (after normalization but without background removal) recovered/smoothed from low-SNR Raman measurements using SG algorithm, FIR filtration, wavelet transform, factor analysis and WE method

	SG algorithm	FIR filtration	Wavelet transform	Factor analysis	WE method
Mean relative RMSE	8.83×10^{-2}	8.81×10^{-2}	8.83×10^{-2}	8.79×10^{-2}	2.05×10^{-2}

In order to clearly see whether the background removal process influences the results, the mean relative RMSE of recovered/smoothed Raman spectra (after normalization but without background removal), using SG algorithm, FIR filtration, wavelet transform, factor analysis and WE method, were compared as shown in Table 3. The mean relative RMSE for WE

method is 23.2%, 23.3%, 23.2%, 23.3% those of SG algorithm, FIR filtration, wavelet transform and factor analysis, respectively. Table 4 shows the comparison in the mean relative RMSE of Raman spectra from bacteria samples (after normalization but without background removal) recovered using SG algorithm, FIR filtration, wavelet transform, factor analysis and WE method. The mean relative RMSE for WE method is 63.3%, 57.8%, 62.9%, 45.0% those of SG algorithm, FIR filtration, wavelet transform and factor analysis, respectively. In both Tables 3 and 4, WE method shows significant improvement compared with other techniques. Therefore, WE method shows much better performance on the raw Raman measurements as well when fluorescence background is not removed.

Table 4. Comparison in the mean relative RMSE of Raman spectra of bacteria samples (after normalization but without background removal) recovered/smoothed from low-SNR Raman measurements using SG algorithm, FIR filtration, wavelet transform, factor analysis and WE method

	SG algorithm	FIR filtration	Wavelet transform	Factor analysis	WE method
Mean relative RMSE	1.58×10^{-2}	1.73×10^{-2}	1.59×10^{-2}	2.22×10^{-2}	1.00×10^{-2}

4. Discussion

Results from phantom samples as in Fig. 3 show that the agreement in peak locations between reference Raman spectra and Raman spectra recovered from low-SNR Raman measurements using WE method as shown in Fig. 3(e) is excellent and spectral shape information is mostly preserved. In Raman spectra recovered using SG algorithm as shown in Fig. 3(a), peak locations are distorted and spectral shape information is lost, because those weak Raman features in spectra with extremely low SNR can be easily smoothed out. FIR method, as shown in Fig. 3(b), fails to distinguish Raman peaks from noise due to the large variance of the noise, thus it shows poor performance in the recovery of the peak locations and spectral shape. Wavelet transform, as shown in Fig. 3(c), shows good performance in noise removal, but important spectral shape information such as the central wavelengths and bandwidths of peaks is lost. The Raman spectra recovered using factor analysis are still noisy, as shown in Fig. 3(d), which suggests this method does not work well in this case. This is likely because the signal and the noise have comparable contributions to the measured Raman spectra.

Results from bacteria samples in Fig. 4 show that the agreement in the locations of those peaks with relatively high intensity between reference Raman spectra and Raman spectra recovered from low-SNR Raman measurements using WE method as shown in Fig. 4(e) is excellent and the spectral shape information is mostly preserved. However, several small peaks are not recovered well, which is not as good as in the recovery of phantom spectra. This is because the Raman signals of bacteria samples are much weaker than those in phantoms. Compared with WE method as shown in Fig. 4(e), the SG algorithm, FIR filtration and wavelet transform, illustrated in Fig. 4(a-c), show much worse results, in which most peak locations are shifted and spectral shape is distorted. The Raman spectra recovered using factor analysis as shown in Fig. 4(d) are still noisy, which suggests this method does not work well in terms of noise removal.

In Fig. 3 and 4, it can be found that the reference spectrum is different for each noise reduction technique. The reason for such a difference in the reference spectra is explained as follows. The test results on a single phantom or bacteria sample was inadequate to represent the performance for all techniques because each technique gives different performance on various phantoms or bacteria samples. To avoid this issue, 25 phantoms and 20 bacteria samples were used and the mean relative RMSE was used to evaluate the overall performance of those techniques. In this sense, the typical cases, i.e. the relative RMSE close to the mean relative RMSE, can effectively represent the performance of different techniques. However, it is impossible to find a phantom or bacteria sample that was the typical case for all five

different techniques, because each technique showed different performance on the same phantom or bacteria. Therefore, five different phantoms or bacteria samples were selected, in which one represented the typical case for each technique.

For bacteria samples, we have tested the recovery of Raman spectra from two other sets of low-SNR measurements with exposure times of 5 s and 10 s in addition to an exposure time of 1 s. The SNRs are 2.09 and 2.87 for low-SNR measurements with exposure times of 5 s and 10 s, respectively. Table 5 shows the comparison in the mean relative RMSE of Raman spectra of bacteria samples (after fluorescence background removal and normalization) recovered from low-SNR Raman measurements (acquired with different exposure time) using SG algorithm, FIR filtration, wavelet transform, factor analysis and WE method. With an increasing exposure time, all methods, i.e. SG algorithm, FIR method, wavelet transform, factor analysis and WE method, yield better performance. WE method always yields the best result among the five methods, while SG algorithm, FIR filtration, wavelet transform and factor analysis show performance similar to each other but considerably worse than WE method.

Table 5. Comparison in the mean relative RMSE of Raman spectra of bacteria samples (after fluorescence background removal and normalization) recovered from low-SNR Raman measurements with different exposure time using SG algorithm, FIR filtration, wavelet transform, factor analysis and WE method

Exposure time	SG algorithm relative RMSE	FIR filtration relative RMSE	Wavelet transform relative RMSE	Factor analysis relative RMSE	WE method relative RMSE
1 s	1.47×10^{-1}	1.54×10^{-1}	1.45×10^{-1}	1.48×10^{-1}	8.21×10^{-2}
5 s	9.78×10^{-2}	9.94×10^{-2}	9.67×10^{-2}	1.10×10^{-1}	7.08×10^{-2}
10 s	8.56×10^{-2}	8.67×10^{-2}	8.33×10^{-2}	1.01×10^{-1}	6.55×10^{-2}

The excellent performance of WE method can be attributed to two factors. One factor is that the synthesis of narrow-band measurements from low-SNR Raman spectra, in which Raman signals are integrated in the wavenumber dimension thus improving the SNR in narrow-band measurements. This works because shot noise dominates in typical Raman measurements [26, 27]. A similar strategy, i.e. integration of Raman signals over time or using a long exposure time in data acquisition, is used more often in practice [28]. The other factor is that WE method takes advantage of prior information about samples contained in Wiener matrix. Note that Wiener matrix is created in the calibration stage, in which Raman spectra with high SNR measured from similar samples are used and associated with narrow-band measurements. Unfortunately, the second factor is also responsible for the limitation of WE method, i.e. the Wiener matrix has to be derived from Raman spectra with high SNR measured from similar samples in the calibration stage prior to spectral recovery from low-SNR measurements. It would work better if the spectral variation across samples is smaller. For this reason, WE method would not work well if the calibration data set is very different from the test data set or when it is impossible to obtain the calibration data set. However, it should be pointed out that the calibration data set is often available in most biomedical applications. This fact has been utilized in many earlier researches in medical diagnostics [29, 30] thus not a problem in these applications.

Compared with other advanced methods, the advantages of our method include its simplicity, short processing time and excellent performance. The iterative three-point zero-order SG filter method [31] is a fully automatic noise reduction method based on SG smoothing. Compared with this method, our method is simpler since it does not need iteration thus would be faster. In addition, our method always shows significant improvement in spectral shape preservation compared with SG filters based methods. For example, the iterative SG method always shows the peak height reduction problem while the method based

on Wiener estimation shows much better performance on peak preservation in Fig. 3 and 4 of the manuscript. Other advanced noise reduction methods based on regularization, e.g. Chi-squared based filters method [32] and matrix-based two dimensional regularization algorithm [33], are more complex and more time consuming than the proposed method due to the iterations required to satisfy the stop criterion. In contrast, our method requires a calibration data set, but the calibration data set is not needed in the test stage for data processing once the Wiener matrix is created, which not only takes advantage the prior information contained in the calibration data set but also accelerates data processing dramatically.

5. Conclusions

In this study, we develop a method based on spectral reconstruction to recover Raman spectra with low signal-to-noise ratio (SNR). Wiener estimation is used in this method to recover the high-SNR Raman spectra from narrow-band measurements that are synthesized from low-SNR Raman spectra. The synthesis of narrow-band measurements from low-SNR Raman spectra eliminates the effect of noise by integrating the Raman signal along the wavenumber dimension, which is followed by spectral reconstruction based on Wiener estimation to recover the Raman spectrum with high spectral resolution. Non-negative principal components based filters are used in the synthesis to ensure that most variance contained in the original Raman measurements are retained. The method was evaluated on 25 Raman measurements from agar phantoms and 20 Raman measurements from bacteria samples. The agreement in peak locations between reference Raman spectra and Raman spectra recovered using WE (Wiener estimation) method was excellent and spectral shape information was mostly preserved. The relative mean root mean square errors (RMSEs) in cases of both with and without fluorescence background removal were small. In contrast, four commonly used de-noising methods, i.e. SG (Savitzky-Golay) method, FIR (finite impulse response) filtration, wavelet transform and factor analysis, showed significantly worse performance. Therefore, WE method represents a new alternative method for noise removal in those applications where short data acquisition yields Raman spectra with low SNR but creating a calibration data set is feasible.

Acknowledgments

The authors would like to acknowledge financial support from Tier 2 grant (Grant No. MOE 2010-T2-1-049) funded by the Ministry of Education, ASTAR-ANR joint grant (Grant no. 102 167 0115) and ASTAR-PSF grant (Grant no. 122-PSF-0012) funded by ASTAR-SERC in Singapore.